Biochimica et Biophysica Acta, 1057 (1991) 258–272

ADONIS 000527289100099L

BBABIO 43362

II. Langmuir-Blodgett monolayer films of the *Rhodopseudomonas viridis* reaction center: determination of the order of the hemes in the cytochrome *c* subunit

Guillermo Alegria and P. Leslie Dutton

Department of Biochemistry and Biophysics, University of Pennsylvania, Philadelpha, PA (U.S.A.)

(Received 19 November 1990)

Key words: Langmuir-Blodgett film; Bacterial reaction center; Photosynthetic bacterium; Chromatophore; Linear dichroism; (*Rps. viridis*)

The Langmuir-Blodgett (LB) film technique has been applied to produce oriented and photo-active films of isolated reaction center cytochrome *c* complexes (RC-cyt *c*) and chromatophore membranes from the photosynthetic bacterium *Rhodopseudomonas viridis*. Linear dichroism (LD) and redox potentiometry have been used to identify the four cytochrome *c* hemes of the RC-cyt *c* complex. Resolved angular orientations of the four hemes in LB films of both isolated RC-cyt-*c* complexes and of chromatophore membranes permit the reduction of the 24 possible arrangements to two. Additional structural and functional information from other sources allows us to propose a model which best accounts for all the available experimental data.

I. Introduction

In recent years, experimental and theoretical research in bacterial photosynthesis has been considerably stimulated by the availability of the X-ray structures for the reaction center proteins (RC) of the bacterial species *Rps. viridis* [1] and *Rb. sphaeroides* [2,3]. Initially the emphasis was placed on the study of the intra-protein reactions of the RC itself, while less attention was given to the reactions involving the cytochrome *c* subunit in the *Rps. viridis* RC-cyt *c* complex. However, more recently the interest in this topic has increased and a number of laboratories have examined different aspects of the structure and function of the tetra-heme subunit [4–7]. One of the most remarkable features in the X-ray structure of the *Rps. viridis* RC-cyt *c* complex is the linear array of the four hemes in the cytochrome *c* subunit. This arrangement, in which each heme has a unique distance and orientation relative to the light-generated electron acceptor $BChl_2^+$, is in sharp contrast with the arrangement suggested from electron paramagnetic resonance spectroscopy and from functional studies for the analogous hemes of *C. vinosum* [8].

A linear sequence of hemes poses interesting questions both at an elementary level, concerning the identification and biological modus operandi of the previously characterized two high- and two low-potential hemes in the array [4,9], and more complex, addressing the elucidation of the mechanism of electron transfer between the hemes and the $BChl_2^+$ as well as between the hemes themselves.

The necessary identification of each heme in the array has been helped by the work of Dracheva et al. [4] and ourselves [6] which demonstrated that, contrary to the notion of two thermodynamically equivalent high-potential hemes and two equivalent low-potential hemes, the two members of each couple have different redox and spectroscopic characteristics. These results were subsequently extended by Nitchke et al. through a com-

Abbreviations: LB, Langmuir-BLodgett; RC, reaction center; RC-cyt *c*, reaction center cytochrome *c* complex; LDAO, lauryldimethylamine *N*-oxide; β-OG, octyl β-glucopyranoside; DPPC, L-α-dipalmitoyl phosphatidylcholine; PL, phospholipid; MOPS, 3-[*N*-morpholino]propanesulfonic acid; Mes, 2-[*N*-morpholino]ethanesulfonic acid; DAD, 2,3,5,6-tetramethyl-*p*-phenylenediamine; TMPD, *N,N,N′,N′*-tetramethyl-*p*-phenylenediamine; PES, *N*-ethylphenazonium ethosulfate; PMS, *N*-methylphenazonium methosulfate; DNAse, deoxyribonuclease; *o*-phen, 1-10-phenanthroline; DQ, duroquinone; CAPS, 3-[cyclohexylamino]-1-propanesulfonic acid; CHES, 2-*N*-cyclohexamino]ethanesulfonic acid; LD, linear dichroism; DR, dichroic ratio.

Correspondence: G. Alegria, B501 Richards Building, Department of Biophysics and Biochemistry, University of Pennsylvania, Philadelphia, PA 19104, U.S.A.

bination of redox potentiometry and EPR spectroscopy of the hemes in the chromatophore membrane [7].

On the functional side, studies indicate that photooxidation of the high-potential hemes occurs in the range from 77–140 K with an efficiency of 30–40% [10,11], in contrast with previous reports [7,12] that this reaction is rendered inactive in the same temperature range. In combination with the structural information, the recent thermodynamical, spectroscopic and kinetic data on the cytochrome *c* subunit suggests that the functional relationship between the hemes and the RC is more complex than previously considered. Theoretical work on these electron transfer reactions incorporating some of the recent findings has already been published [13]; however, more experimental and theoretical work is required before a detailed understanding of the underlying mechanisms is achieved.

In this report we present a detailed analysis of the angular resolution of the four hemes in *Rps. viridis* in the isolated RC-cyt *c* complex and in the chromatophore membrane using the LB film technique in combination with redox potentiometry and linearly polarized spectroscopy. The results are compared with the angular distribution calculated from the X-ray crystal structure to reduce the number of possible arrangements from 24 to two. Additional experimental evidence is used to propose a model that best accommodates the available information. We will compare our results with those obtained by Nitchke et al. [7], by Vermeglio et al. [14] and by Fritzsch et al. [15] with emphasis on the advantages and disadvantages of the different techniques.

II. Materials and Methods

1. Langmuir-Blodgett films

The methodology for the preparation of LB films of isolated RC-cyt *c* complex (from β-OG and PC dispersions) and chromatophore membranes from *Rps. viridis* was was described in the Materials and Methods section of the accompanying manuscript [33].

2. Preparation of non-oriented samples

Determinations of the angle of refraction (see subsection 5) for both, isolated RC-cyt *c* complexes and chromatophore membrane LB films required samples with non-oriented, uniformly distributed pigments. In both cases this was achieved by deposition of a few drops of the preparation on the glass slide and drying under a stream of argon. Polarized and non-polarized absorption spectra of these samples were indistinguishable, thus proving the lack of orientation.

3. Redox titrations and spectroscopic measurements

Redox titrations and spectroscopic analysis with polarized light of the cytochrome *c* hemes in the LB films of isolated RC cytochrome *c* complex and chromatophore membranes were performed as previously described (see accompanying manuscript, [33]).

For measurements of linearly polarized light-induced absorption changes the measuring beam was polarized, while the excitation beam was non-polarized. In all cases measurements were made with the slide immersed in a redox buffer containing 60% glycerol and, unless otherwise specified, with the slide plane at 30° to the measuring beam. All of the experiments with isolated RC-cyt *c* complex LB films were performed with three different LB film preparations; the dichroic ratios and angles reported are average values. Some of the experiments with chromatophore membrane LB films were single determinations.

4. Linear dichroism: theoretical considerations

In this work LD measurements involve two types of absorption band: single linearly polarized transitions like those associated with the Q_x and Q_y transitions of $BChl_2$ and bands containing two nearly degenerate transitions like those of the heme α-bands [11]. LD theory and its applicaitons to biological systems has been reviewed by Hofrichter et al. [16]. Simplified derivations of the equations for linear dipoles are presented below. The analysis of the heme dipoles follows closely that in Ref. 17.

(a) Linear transition dipoles

(i) Perfect orientation. The laboratory reference frame will be referred to as the one defined as follows. The *z*

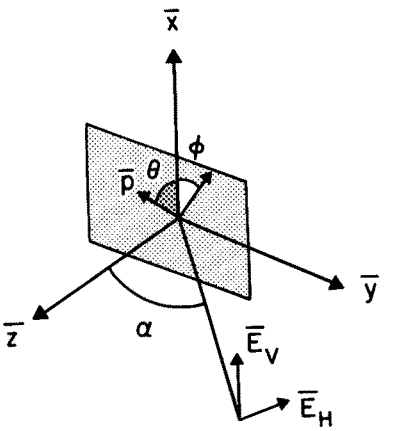

Fig. 1. Linear dipole moment, p_θ, in the left-handed laboratory reference frame defined by the normal to the slide plane (*z* axis), the vertical direction (*x* axis) and the horizontal direction (*y* axis). The angle of the dipole relative to the *x*-*y* plane is denoted θ and the azimuth measured relative to the *x* axis is ϕ. The electric vectors of vertically and horizontally polarized light are shown.

axis corresponds to the normal to the plane of the slide; the x and y axes are defined by the vertical and horizontal directions respectively (see Fig. 1).

We will consider a linear dipole, $\vec{p}$, of a chromophore in an RC molecule whose symmetry axis is aligned with the z axis. Let p_0 be the magnitude of the dipole moment, θ_p be the angle that the dipole makes with the x-y plane and ϕ the azimuthal angle measured clockwise relative to the x axis. The coordinates of the dipole in the laboratory reference frame are then given by:

$$\vec{p} = p_0(\cos\theta_p \cos\phi\hat{x} + \cos\theta_p \sin\phi\hat{y} + \sin\theta_p\hat{z}) \quad (1)$$

where $\hat{x}$, $\hat{y}$ and $\hat{z}$ are unit vectors along the respective axes.

A perfectly oriented sample will be defined as one in which θ_p is the same for all molecules while the azimuthal angles are uniformly distributed in the range $0 \leqslant \phi \leqslant 2\pi$. In the laboratory reference frame a plane-polarized electromagnetic wave can be expressed in terms of vertically and horizontally polarized components as:

$$\vec{E} = \vec{E}_V + \vec{E}_H = E_0\hat{x} + E_0 \cos\alpha\hat{y} + E_0 \sin\alpha\hat{z} \quad (2)$$

where α is the angle between the direction of propagation of the wave inside the sample and the z axis (see Fig. 1).

The dichroic ratio (DR) defined as the ratio of the absorbance with vertically and horizontally polarized light, A_V/A_H, is given by:

$$DR = \frac{A_V}{A_H} = \frac{\int|\vec{p}\cdot\vec{E}_V|^2 \, d\tau}{\int|\vec{p}\cdot\vec{E}_H|^2 \, d\tau} \quad (3)$$

where $d\tau = \sin\theta \, d\theta \, d\phi$.

Substituting Eqns. 1 and 2 into Eqn. 3 and integrating over the interval $0 \leqslant \phi \leqslant 2\pi$ yields:

$$DR = \frac{\cos\theta_p^2}{\cos\alpha^2 \cos\theta_p^2 + 2\sin\alpha^2 \sin\theta_p^2} \quad (4)$$

(ii) Imperfect orientation: order parameter. In practice it is impossible to produce samples with perfect orientation. In a very simple model developed by Fraser [18] and modified by Rafferty et al. [19] the degree of disorder in a sample is expressed in terms of the order parameter, f, defined as follows. The total number of molecules are divided into two subpopulations; a fraction, f, in which all dipoles make the same angle θ_p with the x–y plane but ϕ is uniformly distributed, and a fraction $(1-f)$ in which both θ and ϕ are uniformly distributed. The absorbance with vertically and horizontally polarized light can be written as follows:

$$\begin{aligned} A_V &= fA_{Vp} + (1-f)A_{Vr} \\ A_H &= fA_{Hp} + (1-f)A_{Hr} \end{aligned} \quad (5)$$

where A_{Vp}, A_{Hp} are the contributions to the absorbance from the perfectly oriented fraction and A_{Vr}, A_{Hr} those arising from the randomly oriented fraction. A_{Vp} and A_{Hp} can be obtained from Eqns. 1–3 by integrating over the interval $0 \leqslant \phi \leqslant 2\pi$, while the contributions A_{Vr} and A_{Hr} involve integration over $0 \leqslant \theta \leqslant \pi$ and $0 \leqslant \pi \leqslant 2\pi$. The final expression for the dichroic ratio is:

$$DR = \frac{f\frac{\cos\theta_p^2}{2} + \frac{(1-f)}{3}}{\frac{f\cos\theta_p^2\cos\alpha^2}{2} + f\sin\theta_p^2\sin\alpha^2 + \frac{(1-f)}{3}} \quad (6)$$

As will be discussed later, this simple model enables the estimation of the degree of order in an oriented sample from measurements of DR values for a linear dipole and the knowledge of the angle of refraction.

(b) Non-degenerate linear transitions

Low-temperature spectra of the hemes in *Rps. viridis* RC-cyt *c* complex in solution [11] indicate that the four heme α-bands consist of two non-degenerate transitions. Although the room-temperature absorption spectra of the hemes presented here do not allow a clear resolution of the two components, the polarized absorption spectra of isolated RC-cyt *c* and chromatophore LB films were fitted with two Lorentzian line shapes through a Gauss-Newton fitting procedure using the ASYSTANT + software package (ASYST Software Technologies, Inc. Rochester, NY). In all cases the square of the multiple correlation coefficient was > 0.9. The dichroic ratios of the two components were obtained from the absorption maxima of the fitted amplitudes and the angle that each transition makes with the z axis was obtained using Eqn. 6. Subsequently, the angle between the normal to the heme plane and the z axis was calculated assuming that these transitions lie on the heme plane and are orthogonal to each other. In this case the following relation applies:

$$\cos\theta = \sqrt{1 - \cos\theta_1^2 - \cos\theta_2^2} \quad (7)$$

where θ_1 and θ_2 are the angle that each transition makes with the z axis.

5. Determination of the angle of refraction

The angle of refraction in the films was determined as reported by Rafferty et al. beam polarized parallel to the plane of the substrate. Under these conditions, the

angle of refraction α is determined for several angles of incidence β using the relation:

$$\cos \alpha = \frac{L(0)}{L(\beta)} \tag{8}$$

where $L(\beta)$ is the pathlength of the beam in the film for an angle of incidence β. Because of the uniform distribution of pigments, the pathlength is proportional to the absorbance thus:

$$\cos \alpha = \frac{A(0)}{A(\beta)} \tag{9}$$

The angles of refraction reported in the Results section were averages from determinations with three samples having different absorptions $A(0)$.

6. Baseline subtraction procedure

In order to minimize spectral overlap between cytochromes with similar midpoint potentials and be able to resolve the individual orientations of the four hemes, the following baseline procedure was performed. In the redox potential region from −200 mV to −50 mV all spectra were referred to a baseline at −25 mV where the three hemes with higher midpoints are close to 100% reduced (see Table IV of accompanying manuscript). Thus, their contributions to the absorbance are eliminated. In the redox range from −50 mV to 100 mV all spectra were obtained by subtraction of a reference at 120 mV, where, as before, the two higher midpoint potential hemes are 100% reduced. For the redox span from 200 mV to 320 mV the baseline was taken at 338 mV, where the highest midpoint potential heme is approx. 80% reduced. Finally, the highest midpoint potential heme was characterized using a baseline at 440 mV.

III. Results

1. LD measurements in isolated RC-cyt c complex LB films

(a) Dichroic ratios of the pigments of the RC-cyt c complex molecules in the LB films

Measurements of non-polarized and linearly polarized spectra as a function of the number of layers revealed that, while approximately constant absorption increments per deposition occurred from 1 up to 30 layers, there was a small but steady decrease in orientation with successive depositions after 10 layers. A multilayer with 30 depositions showed a decrease in orientation of approx. 10% relative to that of a single deposition, as judged from the DR values of the different absorption bands (data not shown). Fig. 2 shows typical polarized spectra of a 30 deposition multilayer film of

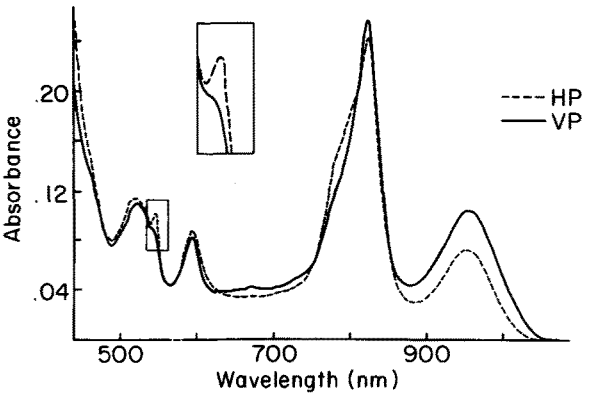

Fig. 2. Polarized spectra of a 30-layer LB film of a β:OG dispersion of RC-cyt *c* complex from *Rps. viridis*. (———) Vertically polarized (VP). (------) Horizontally polarized (HP). The slide was immersed in a 60% glycerol (pH 8.0) buffer containing 20 μM DAD and was placed vertically at 30° to the measuring beam. The redox potential was adjusted to 200 mV by addition of sodium dithionite.

RC-cyt *c* complex in β-OG. The values of the dichroic ratios of the major absorption maxima were: 1.47 ± 0.05 at 960 nm ($BChl_2$ Q_y band), 1.06 ± 0.05 at 830 nm (BChl monomer Q_y band), 0.8 ± 0.03 at 780 nm (BPhl Q_y band) and 0.93 ± 0.04 at 605 nm (mixed chlorophyll Q_x band). As will be shown in the Discussion section, these values are in good agreement with DR determinations using other orientational techniques.

(b) Dichroic ratios of the hemes in the LB films

The dichroic ratio in the cytochrome *c* α-band centered at 556 nm was 0.8 ± 0.035. Resolution of the dichroic ratios of the individual cytochrome *c* hemes in the RC-cyt *c* complex films was accomplished using redox potentiometry. Redox titrations of the kind shown

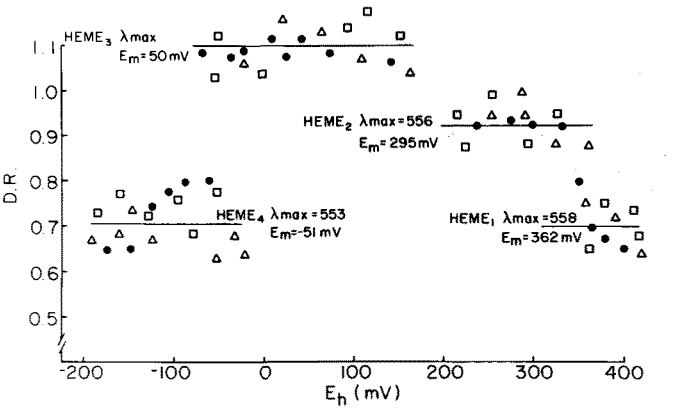

Fig. 3. Dichroic ratio ($DR = A_V/A_H$) as a function of the redox potential in three different LB films (14 layers each) of a β:OG dispersion of RC-cyt *c* complex (△, □, ●). This measuring conditions were as in Fig. 2 except that the redox buffer contained 20 μM each of the following mediators. DAD, PMS, PES, TMPD, pyocyanine, FeEDTA, phenazine and DQ. The DR values were measured at the maxima of the difference spectra obtained through the baseline subtraction procedure described in Materials and Methods. The horizontal lines indicate the average value of the DR obtained from three different preparations.

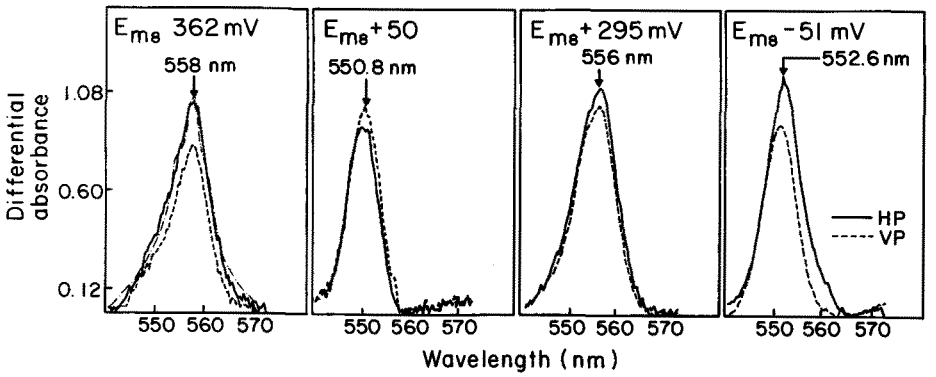

Fig. 4. Resolved polarized spectra of the four hemes in the film (●) used for the titration in Fig. 3. In each case the midpoint potential and the maximum absorbance in the α-band are indicated. The dashed curve overlapping the horizontally polarized spectrum at 362 mV shows a typical fit to the data with two Lorentzian line-shapes. The fitted parameters for all eight spectra are shown in Table I.

in Figs. 12 and 13 of the accompanying manuscript [33] were repeated, except that the absorption spectra were taken with a polarized measuring beam. The orientational resolution of the four hemes is illustrated in Fig. 3, where the dichroic ratios at the maxima in the cytochrome *c* α-band are plotted as a function of the redox potential. In this kind of plot the DR values are not directly related to the Nernst equation, since the orientation of a heme is independent of its redox state. Instead, the shape of the curve is dictated by the resolution of the dichroism of one heme with another (see Materials and Methods section); hence the transitions are precipitous. From this plot the hemes can be divided into two orientational populations: heme 558 and heme 553 with E_{m8} values of 370 mV and −51 mV, respectively, both display DR values of 0.7(±0.05), while hemes 556 (E_{m8} 295 mV) and 551 (E_{m8} 50 mV) have DR values closer to 1 (0.9 ± 0.04 and 1.1 ± 0.04, respectively). Fig. 4 shows the polarized spectra of the four hemes resolved by subtracting DR spectra of one potential region from another. In order to determine the angle of the heme planes, each of these spectra were fitted with two Lorentzian line shapes as indicated in Materials and Methods. A typical fit is shown for the horizontally polarized spectrum at 362 mV. The line shape parameters, dichroic ratios of each component and the angles of each heme normal as determined through Eqns. 6 and 7 are summarized in Table I. The angle of refraction in the isolated β-OG:RC cyt *c* complex LB films shown in Figs. 3 and 4 was determined to be 41° (±10%) for an angle of incidence of 60°.

2. *LD measurements in chromatophore membrane LB films*

Measurement of the spectra of components of the RC-cyt *c* complex in chromatophore membranes is hampered by the lower density of the RC-cyt *c* complex in the membrane and the dominance of the BChl and carotenoid absorbance of the antenna pigment proteins which overlap strongly with the BChl and BPh constituents of the RC, and to a lesser extent with the α-band of the ferrocytochrome *c*. A second method of approach which overcame this problem was the measurement of the polarized flash activated oxidation-reduction difference spectrum of the RC $BChl_2$ and the potentiometrically selected cytochrome *c* hemes. It was found in working chromatophore membranes in general that sucrose density purification led to considerably improved resolution of the spectra (the purification procedure is described in the accompanying manuscript), so this step was included in the work presented here.

TABLE I

Angular characterization of the hemes in LB films of isolated Rps. viridis RC-cyt c complex

Heme	Peak position (nm)		Half-width at half-maximum (nm)		DR_1	DR_2	θ (°) [a]
	λ_1	λ_2	$\Delta\lambda_1$	$\Delta\lambda_2$			
558 nm	558.5	552.6	6.06	7.0	0.67	0.9	63.44
556 nm	556.4	552	5.16	7.0	0.8	1.01	48.94
551 nm	552.9	549	5.8	6.8	1.1	1.21	21.0
553 nm	553.3	550	5.5	4.7	0.87	0.75	59.73

[a] Angles were calculated with $\alpha = 41°$ and $f = 0.65$ using Eqns. 6–7.

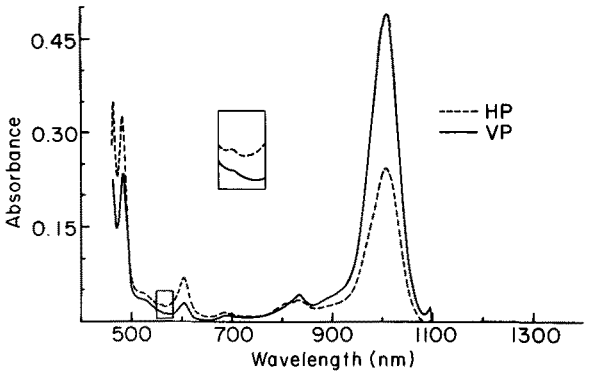

Fig. 5. Polarized spectra of a six-layer LB film of *Rps. viridis* chromatophores at a redox potential of 200 mV adjusted with sodium dithionite in the presence of 30 μM DAD. (———) Vertically polarized (VP). (------) Horizontally polarized (HP). The geometrical configuration for the measurements as as in Fig. 2.

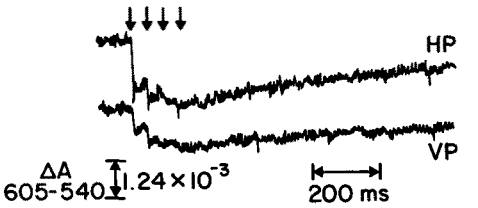

Fig. 6. Polarized light-induced absorption changes at 605 nm in a five-deposition LB film of *Rps. viridis* chromatophores. The cytochrome *c* complement of the reaction center was oxidized by exposing the film to atmospheric oxygen. Under these conditions there was no measurable cytochrome *c* photo-oxidation at 558 nm (data not shown). The DR value was determined by the absorption change after the fourth flash was 0.43. The slide was placed in the 60% glycerol, 10 mM Tris (pH 8.0) buffer. The angle of incidence of the measuring beam was 30°.

(a) Dichroic ratios of the antenna and RC pigment molecules in the chromatophore films

(i) Polarized absorption spectra. Polarized spectra of a multilayer film of purified chromatophore membranes of *Rps. viridis* are presented in Fig. 5. The dichroic ratios of the major bands in the chromatophore spectrum dominated by the antenna pigments were: 1.98 ± 0.034 at 1015 nm (with contributions from the antenna pigments and the Q_y band of $BChl_2$), 1.33 ± 0.04 at 830 nm (BChl monomer Q_y band), 0.46 ± 0.03 at 610 nm (mixture of $BChl_2$ and BChl Q_x band), and 0.71 ± 0.045 at 488 nm (carotenoid). Again, these values are in good agreement with measurements done on chromatophore membranes oriented with other techniques (see Discussion).

(ii) Polarized light-induced difference spectra. The antenna pigments in the chromatophore membrane made the quantitation of DR values for the absorption bands of the pigments of the RC too difficult, and so it was not done. DR values for $BChl_2$ were obtained through polarized light-induced absorption changes associated with the formation of $BChl_2^+$ in films where the cytochrome *c* complement is chemically poised oxidized before excitation; this was done by exposing the film to atmospheric oxygen. Fig. 6 shows the polarized light-induced absorption transients measured at 605 nm; the corresponding DR as determined by the absorption $BChl_2/BChl_2^+$ difference spectrum was 0.43 ± 0.03.

(b) Dichroic ratios of the hemes in the chromatophore films

(i) Polarized absorption spectra. The inset of Fig. 5 shows the location of the cytochrome *c* α-band at 560 nm, for which a value of 0.56 ± 0.03 is obtained. The resolved DR values for the four hemes in a chromatophore LB film through polarized absorption spectra were obtained in an analogous way as with the isolated RC-cyt *c* complex. However, polarized absorption spectra of the chromatophore films were not obtained through the complete redox range. Instead, in this case spectra were obtained at redox potentials of 400 mV, 356 mV, 216 mV, 23 mV and −167 mV. The baselines for each of the hemes were chosen as in the isolated RC-cyt *c* complex films. Fig. 7 shows the resolved polarized spectra together with the dichroic ratios at the maximum of each α-band. It is clear that the same two

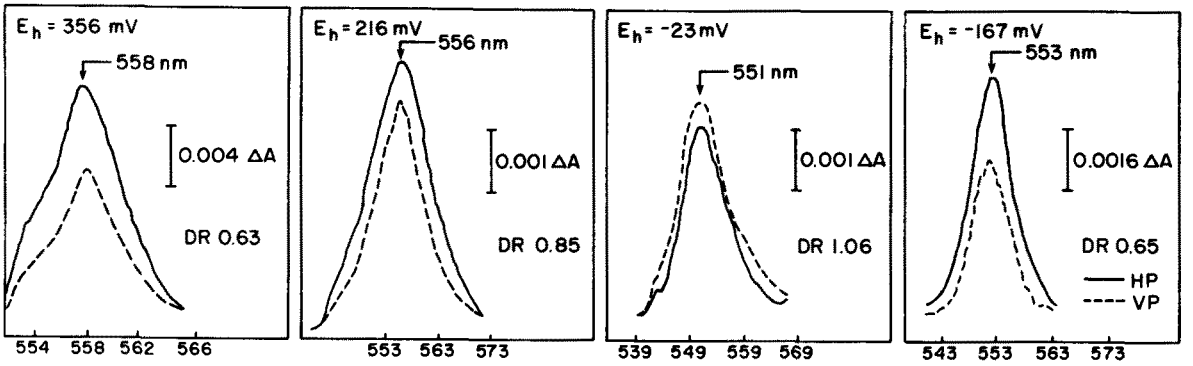

Fig. 7. Resolved polarized spectra of the four hemes in a multilayer LB film of *Rps. viridis* chromatophores. The redox buffer contained 30 μM each of the following mediators: DAD, TMPD, PMS, PES, FeEDTA, phenazine, pyocyanine and DQ. Same geometrical configuration as in Fig. 3. The reference states for the spectra at 356 mV, 216 mV, −23 mV and −167 mV were 400 mV, 330 mV, 100 mV and −50 mV, respectively. The DR values at the maxima are indicated. Fits to the spectra with two Lorentzians yielded the line-shape parameters shown in Table II.

populations determined with isolated RC films are obtained; hemes 558 and 553 have DR values of approx. 0.6, while hemes 556 and 551 have DR values of 0.85 and 1.06, respectively. Again, the eight spectra were each fitted with two Lorentzian line shapes. Table II summarizes the fitted parameters, DR value for each component and the angles of normal to each home plane relative to the z axis.

The angle of refraction for the chromatophore LB films was determined in a similar fashion as that of the isolated RC-cyt c complex films, its value was $40°(\pm 10\%)$ for an angle of incidence of $60°$ and $22.6°(\pm 10\%)$ for an angle of incidence of $30°$.

(ii) Polarized light-induced difference spectra. The individual dichroic ratios of the four hemes in the chromatophore membranes LB films were also determined from measurements of the polarized light-induced reduced minus oxidized spectra. In principle, use of the light-induced cytochrome c spectra should rid the DR determinations of the overlap with the antenna pigments. However, as will be discussed later, the presence of a fully active secondary quinone Q_B in the chromatophore films and the length of the excitation flash did not permit complete elimination of this effect.

The dichroic ratios of each heme were determined by measuring the polarized light-induced spectra of a multilayer film poised at redox potentials of 317, 150, 0 and -100 mV. From Table IV and Fig. 14 of the accompanying manuscript, it is expected that at each one of the chosen potentials the polarized light-induced α-band (reduced minus oxidized) will provide the dichroic ratio of the lowest midpoint potential heme of the ones reduced prior to excitation. The experimental protocol was as follows: after the redox potential was adjusted to 317 mV, vertically and horizontally polarized absorption spectra of the chromatophore film were measured, followed by the polarized light-induced spectra. The potential was then adjusted to the next lower E_h value and the process was repeated. Measurement of the absorption spectra initially and after each potential change provided an idea of the dichroic properties of the reduced hemes and also a control to check that the

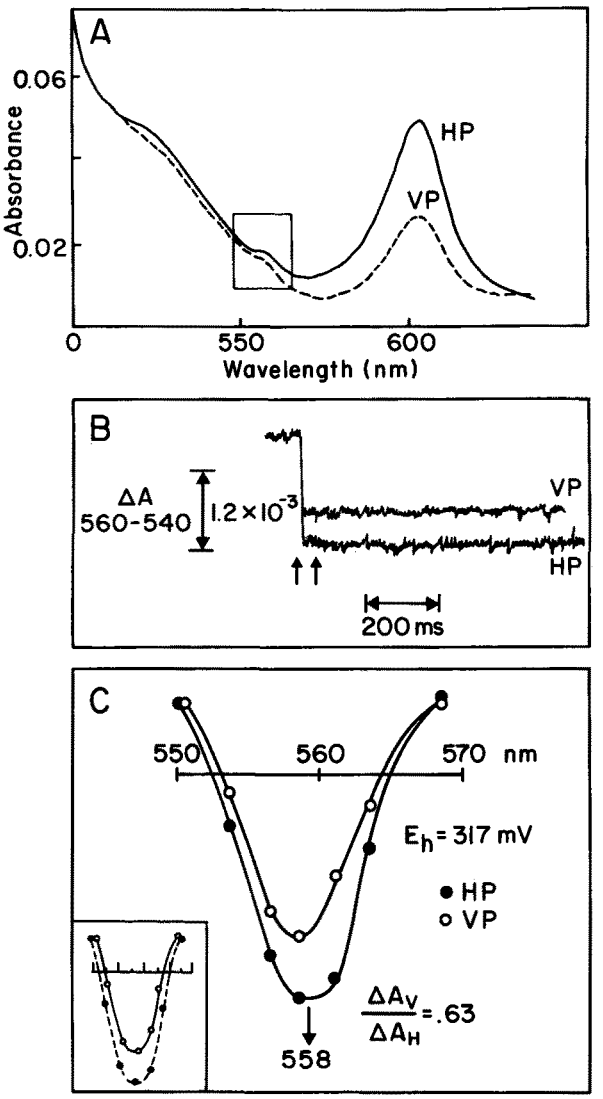

Fig. 8. (A) Polarized absorption spectra of a 6-layer LB film of *Rps. viridis* chromatophores at a redox potential of 317 mV. The redox buffer was the same as in Fig. 7. The rectangle indicates the cytochrome c α-band. (B) Polarized light-induced cytochrome c oxidation at 560 nm (E_h 317 mV) in the same film and conditions as in panel A. The angle of incidence of the measuring beam was 60°. The arrows indicate two successive flashes. (C) Polarized light-induced oxidation spectra obtained through measurements as in panel (B). The DR value at 558 nm is 0.63. The inset shows the polarized spectra under 50% light saturation. Table III summarizes the line-shape parameters of the two Lorentzian fits to the 50% saturation spectra.

TABLE II

Angular characterization of the hemes in LB films of chromatophores of Rps. viridis (absorption spectra)

Heme	Peak position (nm)		Half-width at half-maximum (nm)		DR_1	DR_2	θ (°) [a]
	λ_1	λ_2	$\Delta\lambda_1$	$\Delta\lambda_2$			
558 nm	558.1	552	5.64	5.2	0.65	1.0	74.9
556 nm	556.9	551.9	7.03	6.5	0.7	1.2	60.4
551 nm	552.9	548	5.4	5.02	0.9	1.5	35.4
553 nm	553.9	550	6.4	4.01	0.65	0.93	79.7

[a] Angles were calculated with $\alpha = 40°$ C and $f = 0.76$ using Eqns. 6 and 7.

orientation of the chromatophores remained constant throughout the experiment.

Fig. 8 shows the vertically and horizontally polarized spectra at 317 mV, where only heme 558 is reduced. Panel A shows the absorption spectra of the film in the 500–600 nm region. It seems clear that the film has a DR < 1 in the α-band (area of the spectra enclosed in the box). Panel B shows the light-induced absorption change at 560 nm with horizontally and vertically polarized light. The spectra in Fig. 8C were constructed plotting the absorption changes after the first flash measured at different measuring wavelengths as typified at 560 nm in panel B. The inset in panel C shows the light-induced spectra at 50% light saturation (see Discussion for details). As expected, the light-induced spectra have maxima at 558 nm since at this potential all the other hemes are close to 100% oxidized before excitation. The DR value at the maximum of the α-band is 0.63.

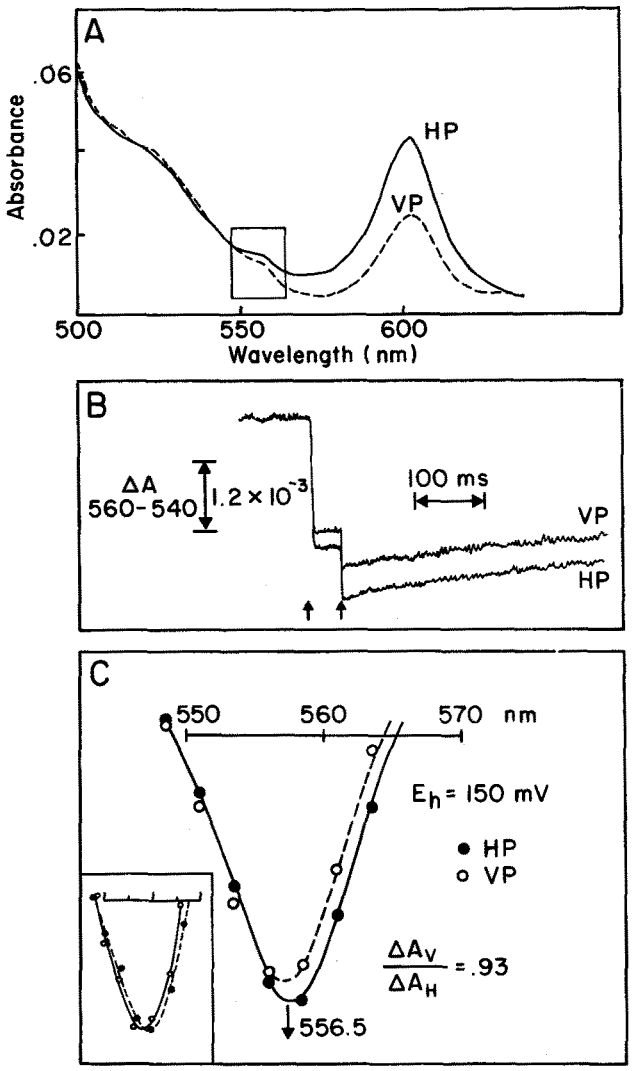

Fig. 9. (A) Polarized absorption spectra at 150 mV measured on the same film and similar experimental conditions as in Fig. 8. (B) Polarized light-induced cytochrome *c* oxidation measured at 560 nm (E_h 150 mV) after two successive flashes. Same geometrical arrangement as in Fig. 8B. (C) Polarized light-induced oxidation spectra obtained by plotting the absorbance extent after the first flash. The DR value at 556.5 nm is 0.93. The inset shows the polarized spectra at 50% light saturation (see Table III for fitted line-shape parameters).

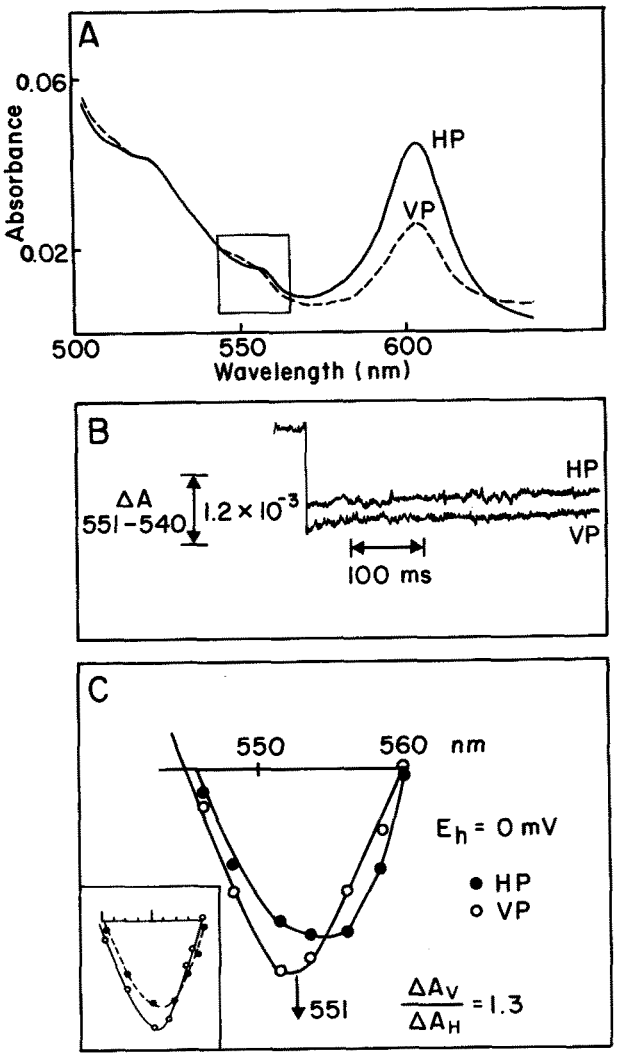

Fig. 10. (A) Polarized absorption spectra in the same film and measuring conditions as in Figs. 8 and 9 at 0 mV. (B) Polarized light-induced cytochrome *c* oxidation at 551 nm (E_h 0 mV) after two flashes. (C) Polarized light-induced oxidation spectra obtained by plotting the absorbance extent after the first flash. The DR value at 551 nm is 1.3. Inset shows the spectra obtained at 50% light saturation (see Table III for fitted line-shape parameters).

Fig. 9 shows the corresponding dichroic behavior at 150 mV, where hemes 558 and 556 are reduced before excitation. As before, panel A shows the polarized absorption spectra of the film, the α-band region in this case contains contributions from both hemes. The light-induced signals at 150 mV are shown in panel B, where the double photo-oxidation step after first and second flashes demonstrates the functionality of both high potential hemes in the film. Furthermore, a plot of the absorption change after the first flash peaks at 556 nm (panel C) with a DR value of 0.93 at the maximum.

The inset in panel C shows the polarized spectra at 50% light saturation.

Fig. 10 shows the results of the dichroic behavior of the cytochrome *c* complement in the same chromatophore film as in the previous two figures poised at 0 mV. Again, from the fast equilibration between the hemes demonstrated in the accompanying manuscript, at this potential the absorption after the first flash is expected to arise from heme 551 (the lowest-potential heme in the reduced state prior to excitation). Fig. 10A shows the polarized absorption spectra of the film. It can be seen that the absorbance at approx. 551 nm shows a slightly higher amplitude with vertically polarized light, i.e., DR > 1. Fig. 10B and C confirms this result; the value of the DR at 551 nm from Fig. 10C is 1.3. As before, the inset in panel C shows the spectra obtained at 50% light saturation.

Fig. 11 shows the results of the equivalent DR study of the cytochrome *c* complement in the same chromatophore LB film at −100 mV. The features of the polarized absorption spectra in the α-band (Fig. 11A) are more difficult to interpret because at this potential the four hemes are close to being 100% reduced and their bands overlap. As for the previous hemes, Fig. 11B and C show the polarized light-induced absorption changes associated with the cytochrome acting as donor to $BChl_2^+$, heme 553 in this case. The DR value measured at 553 nm is 0.6. It is clear from the absorption spectra in the A panels of Figs. 8 to 11 that the orientation of the film remained essentially unchanged throughout the experiment.

In summary, the polarized light-induced cytochrome *c* oxidation spectra in the chromatophore LB films reveals two populations, each comprising a high- and a low-potential heme: hemes 558 (E_{m8} 370 mV) and 553 (E_{m8} −51 mV) with DR values of 0.6, and hemes 556 (E_{m8} 295 mV) and 551 (E_{m8} 50 mV) with DR 0.93 and 1.3, respectively. The angle that each heme plane makes with the *z* axis was calculated in a similar fashion as previously described. However, due to the limited number of data points in each spectra, the fitting of these curves with two Lorentzians was done by constraining the peak positions to be the average values from the two sets of data in Tables I and II. Table III summarizes the Lorentzian parameters, DR ratios for each component and the calculated angles.

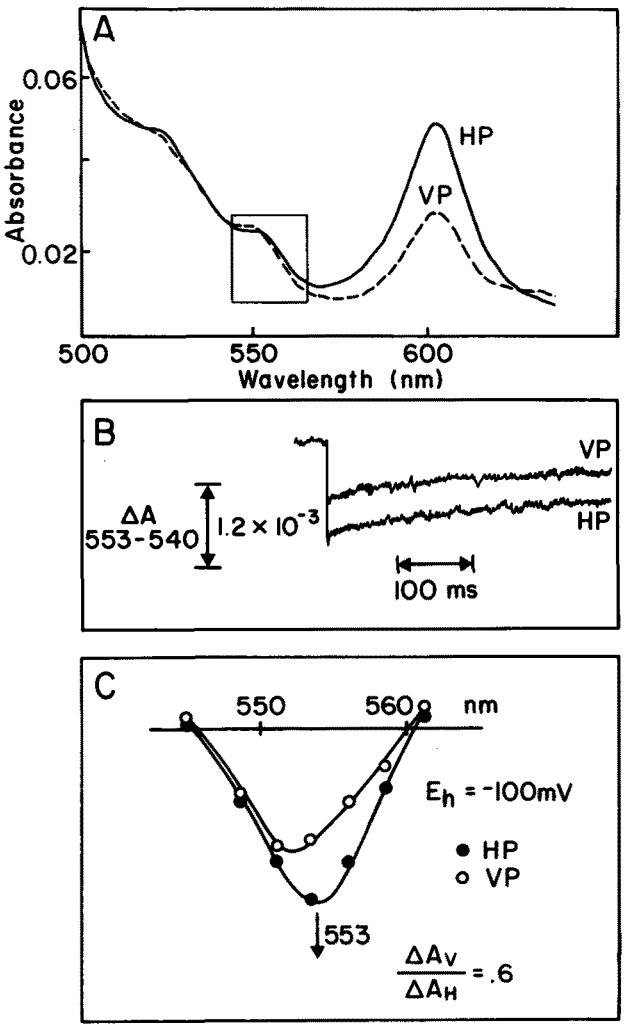

Fig. 11. (A) Polarized absorption spectra of the film used in Fig. 10 at −100 mV. (B) Polarized light-induced cytochrome *c* oxidation at measured at 553 nm (E_h −100 mV). (C) Polarized light-induced oxidation spectra obtained by plotting the absorbance change after the first flash. The DR value at 553 nm is 0.6 (see Table III for line-shape parameters).

TABLE III

Angular characterization of the hemes in LB films of chromatophores of Rps. viridis (light-induced spectra)

Heme	Peak position (nm) [a]		Half-width at half-maximum (nm)		DR_1	DR_2	θ (°) [b]
	λ_1	λ_2	$\Delta\lambda_1$	$\Delta\lambda_2$			
558 nm	558.3	552.3	7.03	5.4	0.72	0.95	71.44
556 nm	556.6	552	5.21	5.3	0.81	1.37	51.57
551 nm	552.9	548.5	5.1	5.2	1.5	1.1	33.7
553 nm	553.3	550	5.1	6.02	0.69	0.93	77.17

[a] Peak positions are average values from Tables I and II.
[b] Angles were calculated with $\alpha = 40°$ and $f = 0.76$ using Eqns. 6 and 7.

For the purpose of simplifying the discussion, the four hemes will be henceforth identified as follows: hi1 (E_{m8} 370 mV, λ_{max} 558), hi2 (E_{m8} 295 mV, λ_{max} 556), lo1 (E_{m8} 50 mV, λ_{max} 551) and lo2 (E_{m8} −51 mV, λ_{max} 553).

IV. Discussion

1. Orientation of the RC-cyt c complex molecules in the LB films

(a) Order parameter of the isolated RC-cyt c complex LB films

The dichroic ratios of all the absorption bands in the spectra shown in Fig. 3 are in good agreement with those previously reported using isolated RC-cyt *c* complexes oriented in squeezed polyacrylamide gels and in single crystals [20,21]. This indicates that in the three systems the optical axis of the RC-cyt *c* molecules exhibits a similar average orientation relative to the *z* axis in the laboratory reference frame. Since the optical axis corresponds to the longitudinal axis of the RC-cyt *c* complex molecule, known to span the membrane in the native system, the plane of the slide can be thought of as equivalent to the membrane plane.

The order parameter, f, of the isolated RC-cyt *c* complex films can be estimated through Eqn. 6 in the Materials and Methods section using the DR value for the 960 nm band which corresponds to a single linearly polarized dipole (that of $BChl_2$) and the angle of refraction α. Substituting the values of 1.47 for DR and 41° for α, f can be expressed in terms of θ as:

$$f = -0.156/\{(-0.714)(\cos(\theta)^2)+0.476\}$$

A plot of this function shows that the minimum value of f consistent with its definition as a number $0 \leqslant f \leqslant 1$ is approx. 0.65. Thus, within the simple model used for the estimation of the degree of orientation of the LB films, this means that at least 65% of the molecules have their optical axis oriented at the same angle relative to the slide plane and 35% are uniformly distributed.

In the absence of additional information, the dichroic ratios presented in this work are insufficient to further characterize the angular distribution of the molecular axes relative to the plane of the slide. However, comparisons between DR values in the LB films and those obtained in oriented membranes for which axial distributions have been specified through X-ray diffraction [23] indicate that the degree of order in the LB films translates into a spread of the molecular axes of the RC-cyt *c* complex (referred to as mosaic spread) of no more than 15° away from the normal to the plane of the slide. Therefore, the assignment of the plane of the slide as equivalent to the membrane plane seems justified.

(b) Order parameter in the chromatophore membrane LB films

Polarized spectra of the chromatophore LB film compare favorably with those of membranes oriented using magnetic fields, air drying and through velocity gradients [24,25]. X-ray data on chromatophore membranes oriented by drying on quartz slides shows that the lipid bilayer orients parallel to the plane of the slide [23]. In view of the excellent agreement in the DR values between these systems and the LB films we conclude that in the latter the membrane plane is also parallel to the slide. It thus follows that the optical axis of the RC-cyt *c* complex orients perpendicular to the plane of the slide. The order parameter of the chromatophore LB films was determined in a similar fashion as that for the isolated RC-cyt *c* films. However, the dichroic ratio used was that obtained through the polarized light-induced absorption changes at 605 nm (DR = 0.43). The angle of refraction α in this case was 22.6° for an angle of incidence of 30°. When these values are substituted in Eqn. 6 and f is expressed as a function of θ, the following equation is obtained:

$$f = 0.19/\{(-0.38)(\cos(\theta)^2)+0.25\}$$

As before, a plot of this equation shows that the minimum value of f in the range $0 \leqslant f \leqslant 1$ is 0.76. This compares with typical values of 0.75 for membranes of *Rps. viridis* oriented in magnetic fields and of *Rb. sphaeroides* oriented by drying suspensions on glass slides [19,20]. Furthermore, the chromatophore films show an improved order of approx. 10% over isolated RC-cyt *c* complex LB films. This represents a mosaic spread of approx. 12°.

2. Orientation of the heme planes in the LB films

(a) Heme angles in the isolated RC-cyt c complex films

The angle that each heme plane makes with the normal to the slide was calculated using Eqns. 6 and 7 with $\alpha = 41°$, $f = 0.65$ and the DR values obtained as described in the Results section (see Table I). Uncertainties in the angle of refraction and the DR values correspond to ±10° uncertainties in θ. For an order parameter $f = 0.9$, all the angles decrease by approx. 10°. since the value of 0.65 is a lower limit to the order parameter, the angles are likely to be overestimated.

(b) Heme angles in the chromatophore LB films

The angles of the heme planes in the chromatophore membrane LB films were calculated from the dichroic ratios in a similar way as described above for the isolated RC-cyt *c* complex films, only in this case the order parameter was 0.76 and $\alpha = 40°$. The values presented in Table II are those calculated from the absorption spectra in Fig. 7. Again, they represent max-

imum values (these values would be approx. 10° smaller for an approx. 10% increment in the order parameter).

As was mentioned in the Results section, the advantage of the light-induced DR measurements over the absorption spectra is the elimination of the overlapping bands from the antennas and carotenoids. In contrast with the observation that the dichroic ratios for the isolated RC-cyt *c* complex LB films do not exhibit transitions from DR > 1 to DR < 1 in any of the four α-bands, Fig. 10 indicates that for heme 551 nm such a transition does occur. Furthermore, close inspection of all four spectra (panels C, Figs. 8–11) reveals that larger variations in DR are observed in this case relative to the absorption spectra of isolated RC-cyt *c* complex films. Although this may be the result of a better resolution in the absence of spectra overlap, these differences are in part due to the fact that a long excitation flash has the potential to produce multiple turnovers. Indeed, measurements of the extent of cytochrome *c* photo-oxidation in chromatophores in solution in the presence and absence of *o*-phenanthroline to inhibit the Q_A to Q_B electron transfer revealed a maximum of 15% double turnovers, However, use of *o*-phenanthroline was avoided in the LB film experiments because long exposure times (approx. 30 min) to the required concentrations of this inhibitor caused irreversible loss of the signal.

Thus, under the conditions of our measurements, the light-induced DR determinations contain some spectral overlap, since the absorption change after a single flash contains contributions from two hemes. We observed that working at 50% light saturation the double turnover effect is completely eliminated. The insets of panels C of Figs. 8–10 show the corrected spectra. It is clear that in all three cases, although the spectra have approximately the same dichroic properties, the variations in DR along the α-band are less pronounced when the double turnover effect is eliminated. The spectra at −100 mV were obtained at 50% saturation, since at this potential Q_B is completely reduced before excitation and is not capable of acting as a two electron acceptor. Calculations of the heme angles were performed using the corrected spectra as described in the Results section, these are summarized in Table III.

Tables I, II and III clearly indicate that the three types of determination yielded very similar results. It should be emphasized that, while hemes 558 and 553 are almost parallel to each other (with θ closer to 90°), the two intermediate ones exhibit an average differential angle of 23° with the plane of heme 551 less tilted than that of heme 556.

2. *Determination of the heme order in the cytochrome c subunit*

With the knowledge of the angular distribution of the heme planes relative to the membrane plane in addition to their spectroscopic resolution, it is possible to establish a connection with the X-ray crystal structure to identify each heme in the linear array. The main contribution from the LB film work is providing the unambiguous assignment of the angular disposition of the hemes both in the isolated RC-cyt *c* complexes and chromatophore LB films. In both cases the highest- and lowest-potential hemes have their planes considerably out of the membrane plane, while the planes of the two intermediate ones are closer to the membrane plane. Hence, there are two angular populations, each comprising one high- and one low-potential heme. Judging from the X-ray crystal structure we can tentatively draw up a sequence in which the highest- and lowest-potential hemes are placed at the ends of the linear array and the others represent the two central hemes. Fig. 12 shows

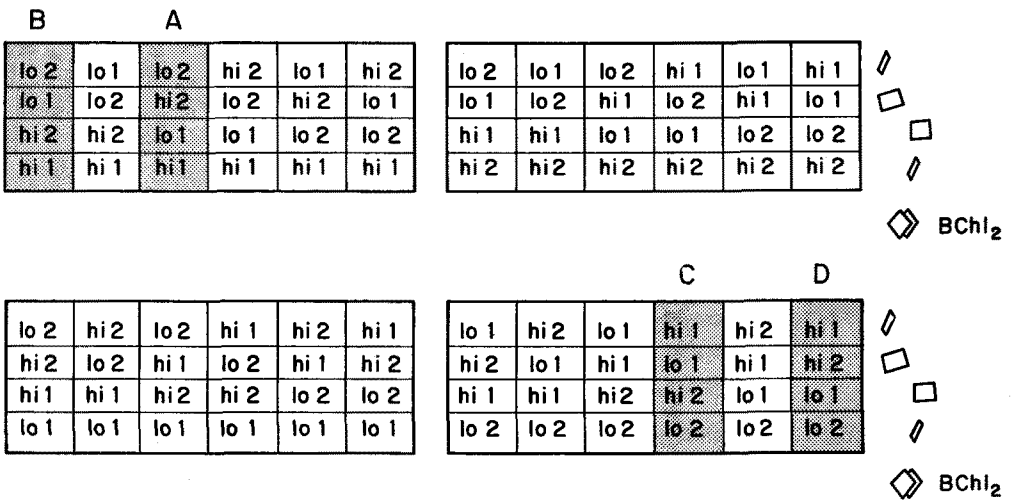

Fig. 12. Twenty-four possible arrangements of the four hemes in the *Rps. viridis* RC-cyt *c* complex. The hemes are denoted as follows: hi1 (370 mV, 558 nm), hi2 (295 mV, 556 nm), lo1 (50 mV, 551 nm), lo2 (−51 mV, 553 nm). The location of the hemes relative to the special pair $BChl_2$ is indicated.

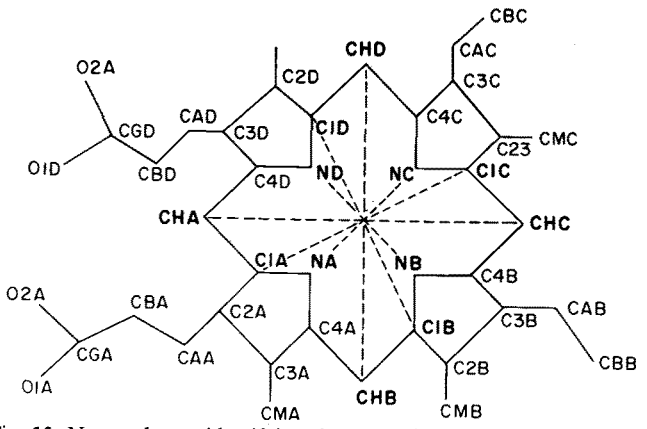

Fig. 13. Nomenclature identifying the atoms in the heme porphyrin ring. The dotted lines connect the atoms used in the calculation of the angle of each heme plane relative to the C2 symmetry axis.

that only 4 out of the 24 possible arrays satisfy this requirement. These are:

(A) RC-hi1, lo1, hi2, lo2
(B) RC-hi1, hi2, lo1, lo2
(C) RC-lo2, hi2, lo1, hi1
(D) RC-lo2, lo1, hi2, hi1

In order to narrow down the number of possibilities, we calculated the angle that each heme makes with the C2 symmetry axis using the X-ray coordinates for the atoms in each porphyrin ring. Fig. 13 illustrates the nomenclature used to identify each atom in the ring. Angular calculations were done in three different ways: (i) Two vectors in the heme plane were defined as $\vec{N}_1 = \vec{N}_A - \vec{N}_C$ and $\vec{N}_2 = \vec{N}_B - \vec{N}_C$, where $N_{A,D}$ is the group of nitrogens in coordination with the Fe atom. A vector perpendicular to $\vec{N}_1$ and $\vec{N}_2$ was then generated through the product $\vec{h} = \vec{N}_1 \times \vec{N}_2$ and the angle of the normal to the heme with the C2 axis calculated through the normalized scalar product

$$\frac{\vec{h}\cdot\hat{z}}{|\vec{h}\cdot\hat{z}|},$$

where $\hat{z}$ is a unit vector along the molecular axis. (ii) In a similar manner, the angle was calculated using the group of atoms CH_A, CH_B, CH_C and CH_D. (iii) The third determination was done using the coordinates of atoms C_{1A}, C_{1B}, C_{1C} and C_{1D}.

These results are summarized in Table IV, which points out that, while the proximal and distal hemes (numbered 1 and 4 in the table) are almost parallel to each other, the intermediate ones (2 and 3) show an average differential angle of 19.8°, with the plane of heme 2 closer to the membrane plane. Comparison of the values in Tables I to IV shows that the experimental angles are significantly higher than the calculated ones. As expressed in section 2, this difference is due mostly to the uncertainty in the order parameter. However, the two angular populations are clearly identifiable. Furthermore, it can be appreciated that in the three experimental determinations the two external hemes are nearly parallel to each other whereas the intermediate ones show an average 23° differential angle. From this result it can be concluded that the heme with its plane more parallel to the membrane plane, heme lo1, corresponds to the second heme away from $BChl_2$ in the X-ray crystal structure. Arrangements (A) and (D) are therefore the only ones that can account for this result.

The kinetic properties of the electron transfer reactions from the two high-potential hemes to $BChl_2^+$ [4,5] can be used to rule out arrangement (D). Indeed, the submicrosecond reduction of $BChl_2^+$ by heme 558 would be difficult to accommodate by arrangement (D) in which the distance between the first high-potential heme and $BChl_2$ is in excess of 40 Å. Furthermore, as has been shown through optical measurements at room temperature [4,5], the reduction of $BChl_2^+$ by heme 558 nm is followed by electron transfer from heme 556 to heme 558, placing the former further away from $BChl_2$. Arrangement (A) can accommodate these observations.

After our first publication on the issue of the order assignment of the hemes in the *Rps. viridis* cytochrome *c* subunit [6], Nitchke et al. addressed the problem by applying EPR spectroscopy on chromatophore membranes oriented on mylar [7]. It is interesting to compare their results with ours. In the EPR study the four hemes were resolved electrochemically and magnetically; the angular dependence of the g_z signal of each heme was used to determine the individual orientation of the heme planes relative to the membrane. These results yielded the same four possible arrangements proposed above. In addition to the angular distribution, these authors measured the low-temperature electron transfer properties of the cytochrome *c* complement under steady-state illumination at redox potentials where all the hemes were reduced prior to excitation. By looking at the amplitudes and shifts of the g_z signals at 4 K, it was concluded that, under these conditions, heme E_{m8} 20 mV (551 nm) is likely to be the electron donor to $BChl_2^+$. Upon warming the samples, they

TABLE IV

Angular characterization of the hemes in the cytochrome c subunit of Rps. viridis RC-cyt c complex using X-ray coordinates

Heme [a]	Angle of the normal to the heme plane rel. to C2 axis (°)			
	atoms N_{A-D}	atoms CH_{A-D}	atoms Cn_{A-D} [b]	average
4	54.21	55	54.38	54.53
3	40.58	40.49	41.1	40.7
2	20	21.39	21.2	20.86
1	55.37	56.47	55.88	55.9
$BChl_2$				

[a] Position of each heme relative to $BChl_2$.
[b] $n = 1, 2, 3, 4$.

observed the formation of a g_z signal associated with the oxidation of heme E_{m8} −80 mV (553 nm. From these observations they tentatively identified heme −80 mV as the fourth heme away from $BChl_2$ and hence arrived at arrangement (A) as the most plausible one.

One of the advantages of the EPR spectroscopic study over the optical analysis is the fact that the EPR signals of the high-potential hemes (with a midpoint potential difference of only 75 mV) are more clearly resolved. However, the opposite is true for the low-potential hemes (midpoint difference of > 100 mV). On the other hand, angular determinations using the amplitude of the g_z signals as a function of the angle between the slide plane and the direction of the magnetic field did not resolve intermediate orientations between 45° and 90° and the comparison with the structural data is not as fruitful. The additional information obtained by the EPR analysis of the low-temperature photochemistry has recently been challenged by a more detailed EPR study of the electron donation by the high-potential hemes at low temperature [10]; Nitschke et al. reported no high-potential heme photo-oxidation at low temperatures, while Hubbard et al. [10] observed photo-oxidation of both high-potential hemes at 15 K. Furthermore, these workers argued that at redox potentials at which all the hemes are reduced prior to illumination, heme 556 and not heme 551 is the one acting as an electron donor to $BChl_2^+$. This issue is still not resolved because the g_z signal of hemes 556, 553 and 551 overlap and the assignment is still ambiguous. However, optical studies dealing with this problem are in progress in several laboratories [11,27].

Nitschke et al. [7] provided further experimental evidence unique to the EPR approach relevant to the identification of the heme order by analysis of the magnetic interactions between the hemes in the *Rps. viridis* RC-cyt *c* complex. They presented evidence suggesting that the lower of the two high-potential hemes (heme 556) interacts with both low-potential hemes, while no appreciable interaction is observed between the two members of the low-potential couple. However, due to overlap of the EPR signals of all the hemes except that of the highest midpoint potential one, magnetic interactions alone could not unequivocally determine each heme's nearest neighbors. Nevertheless, it can be argued that these observations, while being accommodated by model (A), cannot be readily accounted for by model (D).

Similar results were reported by Tiede et al. [8] in a study of magnetic interactions between the hemes in *C. vinosum*. These workers observed no interactions between the high-potential cytochromes or the low-potential cytochromes, while high potential–low potential interactions were clearly identified. This would suggest an analogous distance arrangement of alternating high–low-potential hemes in *C. vinosum* and *Rps. viridis*. However, Tiede et al. proposed a configuration in which the members of each redox couple are parallel to each other and the low-potential and high-potential hemes are oriented parallel and perpendicular to the membrane, respectively. Since the structure of the RC-cyt *c* complex of *C. vinosum* is not known, the source of the discrepancy cannot be resolved at this point. Nonetheless, a more adequate comparison requires the resolution of each individual heme, absent in Ref. 8. In this regard we have preliminary evidence for the electrochemcial, optical and orientational resolution of the two high-potential hemes in LB films of *C. vinosum* chromatophores [28]. We observe that in these systems the midpoint potentials and absorption maxima in the Soret band of the high potential hemes are clearly resolved: (389 mV, 423 nm) and (325 mV 421 nm), respectively. In addition, the heme planes appear to have different orientations; heme 423 nm is almost parallel to the membrane plane and heme 421 nm is in an almost perpendicular orientation. Although more work is required for a complete characterization of the four hemes, these preliminary results suggest that Tiede's original proposal is not accurate. Furthermore, the orientation of the high-potential hemes in *C. vinosum* appears to be opposite to the one encountered in *Rps. viridis*; the highest-potential heme. perpendicular to the membrane in *Rps. viridis*, is parallel to the membrane in *C. vinosum*.

Another line of evidence lending support to arrangement (A) comes from theoretical work by Gunner et al. [29]. These workers calculated the electrostatic potential throughout the *Rps. viridis* RC-cyt *c* complex solving the Poisson-Bolzmann equation including the charges of acidic and basic residues on the surface of the cytochrome subunit, energies of solvation, nature of the axial ligand sand inter-heme electrostatic interactions. Their calculated midpoints are in excellent agreement with the assignment of model (A).

More recently two independent studies on the heme assignment in *Rps. viridis* have been published [14,15]. In Ref. 14 Vermegio et al. arrived at arrangement (A) through a study of the low-temperature linear dichroism of isolated RC-cyt *c* complex oriented in squeezed polyacrylamide gels. This work presents clearly resolved LD spectra of three of the hemes (that of heme −80 mV overlapped with the BPh absorption band). The heme ordering was assigned by comparing the experimental data with a theoretical calculation of the LD spectra using the crystallographic coordinates. These workers found that only array (A) can account for their spectroscopic evidence in conjunction with a theoretical claculation of the LD using the X-ray coordinates. Their conclusion is based on the presence of two transitions in the spectrum of heme 556 exhibiting opposite LD (only reproducible with the coordinates of the third heme away from $BChl_2$). However, Kaminskaya et al.

[11] have shown that the Q_x and Q_y transitions of all four hemes are resolvable in the low-temperature absorption spectra of isolated reaction centers. The polarization properties of these transitions are yet to be characterized.

In Ref. 15, Fritsch et al. also arrived at arrangement (A) through analysis of polarized absorption spectra of redox poised crystals. A puzzling observation in this paper is that, in spite of the equivalency of the first and fourth hemes relative to the C2 symmetry axis of the RC in the crystal structure, the polarized spectrum of the lowest-potential heme (number 4 in Table IV) does not exhibit dichroism, while that of the highest-potential one (number 1 in Table IV) exhibits the highest DR value.

Finally, it is worth commenting on the implications of the structural arrangement of the four hemes to the mechanism of electron transfer as well as their physiological relevance. Gao et al. [27] showed that the low-temperature recombination rates for the reactions cyt $hi1^+ Q_A^-$ and cyt $hi2^+ Q_A^-$ appear to be activationless, with the rate for the former only 10-fold faster than the latter. This is a surprising result in view of the expected decrease in rate of approximately thirteen orders of magnitude for the additional 30 Å separation between heme hi2 and Q_A implied by arrangement (A). Gao et al. suggest that a possible explanation is the involvement of the intervening low potential heme extending the wave function of heme hi2 in a superexchange fashion. However, additional experimental evidence is required to understand the role of the intervening low-potential heme, including a detailed characterization of the temperature dependence of the forward inter-heme electron transfer from heme hi2 to hi1. Unresolved questions regarding the heme-$BChl_2^-$ electron transfer mechanisms have been pointed out by Kaminskaya et al. [11]. This work presents evidence that, while cyt lo1 remains 100% photoactive at 77 K, cyt hi1 is only 20% active, an observation still unexplained if, as implied by arrangement (A), photo-oxidation of cyt lo1 occurs via cyt hi1.

The physiological role of the cytochrome *c* subunit is unclear; Shill et al. [30] have shown that heme 558 (cyt hi1), interacts with a soluble c_2 type cytochrome and suggested that this is the pathway for cyclic electron transfer in *Rps viridis*. On the other hand, it has been proposed that the low-potential hemes may be involved in non-cyclic electron flow [31,32]. It has also been suggested [9] that the existence of a subunit with multiple redox centers may serve to efficiently couple the RC not only with $n = 1$ redox couples but substrates with $n = 2$, 3 or even 4 redox transitions (sulfur compounds, for example). However, no clear evidence has yet been published to support these notions.

Fig. 14 summarizes the structural spectroscopic and electrochemical characteristics of the order assignment

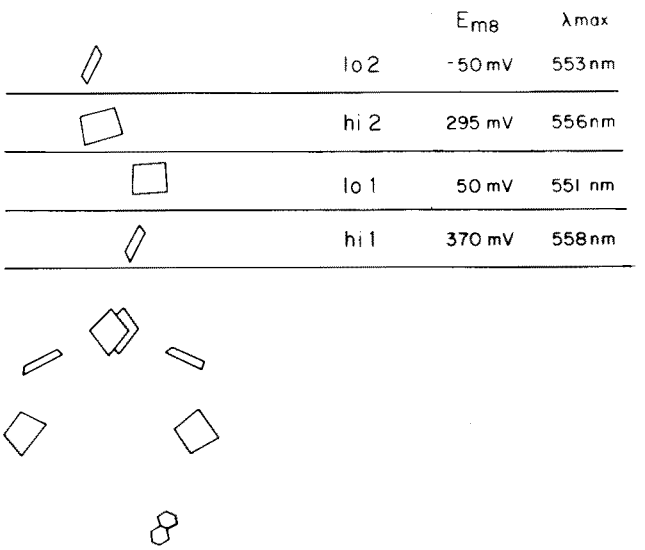

Fig. 14. Model of the heme arrangement that best accommodates the available structural and experimental evidence. The midpoint potential and α-band maximum of each heme are indicated.

consistent with the experimental evidence presented here in addition to the information from the X-ray crystal structure and EPR spectroscopy. It has to be pointed out that, in spite of the agreement in the assignment from the four independent determinations [6,7,14,15], further characterization is required before it can be firmly established. In particular elucidation of the low temperature electron transfer pathway at redox potentials where all the hemes are reduced prior to excitation. EPR experiments done under these conditions reported in Refs. 7 and 10 have yielded conflicting conclusions regarding the location of the low-potential hemes. Also required is experimental evaluation of redox and/or spectroscopic interactions between the hemes.

Acknowledgment

This work was supported by Grant GM 41048-02 from the United States Public Health Service.

References

1 Michel, H. (1982) J. Mol. Biol. 158, 567–572.
2 Allen, J.P., Feher, G., Yeates, T.O. Rees, D.C., Deisenhofer, J. et al. (1986) Proc. Natl. Acad. Sci. USA 83, 8589–8593.
3 Chang, C.H., Tiede, D.M., Tang, J., Norris, J.R. and Schiffer, M. (1987) in Progress in Photosynthesis Research (Biggins, J., ed.), Vol. 1, pp. 371–374, Kluwer, Dordrecht.
4 Dracheva, S.M., Drachev, L.A., Zaberezhnaya, S.M., Konstantinov, A.A., Semenov, A.Y. and Skulachev, V.P. (1986) FEBS Lett. 205, 41–46.
5 Shopes, R.J., Levine, L.M.A., Holten, D. and Wraight, C.A. (1987) Photosynth. Res. 12, 165–180.
6 Alegria, G. and Dutton, P.L. (1987) in Cytochrome Systems (Papa, S., Chance, B. and Ernester, L., eds.), pp. 601–606, Plenum Press, New York.
7 Nitschke, W. and Rutherford, A.W. (1989) Biochemistry 28, 3161–3167.

8 Tiede, D.M., Leigh, J.S. and Dutton, P.L. (1978) Biochim. Biophys. Acta 503, 524–544.
9 Dutton, P.L. (1986) Encyclopedia of Plant Physiology, Vol. 19 (Staehlin, L.A. and Antzen, C., eds.), pp. 197–237, Springer, Heidelberg.
10 Hubbard, J.A.M. and Evans, M.C.W. (1989) FEBS Lett. 244, 71–75.
11 Kaminskaya, O., Konstantinov, A.A. and Shuvalov, V.A. (1990) Biochim. Biophys. Acta 1016, 153–164.
12 Chance, B., Kihara, T., De Vault, D., Hildreth, W., Nishimura, M. and Hiyama, T. (1969) in Progress in Photosynthesis Research Vol. 3 (Metzner, H., ed.), pp. 1321–1346, Tübingen.
13 Bixon, M. and Jortner, J. (1986) FEBS Lett. 200, 300–308.
14 Vermegio, A., Richaud, P. and Breton, J. (1989) FEBS Lett. 243, 259–263.
15 Fritsch, G., Buchanan, S. and Hichel, H. (1989) Biochim. Biophys. Acta 977, 157–162.
16 Hofrichter, J. and Eaton, W.A. (1976) Annu. Rev. Biophys. Bioeng. 5, 511–560.
17 Tiede, D.M. (1987) Biochemistry 26, 397–410.
18 Fraser, R.B.B. (1953) J. Chem. Phys. 21, 511–515.
19 Rafferty, C.N. and Clayton, R.K. (1979) Biochim. Biophys. Acta 546, 189–206.
20 Rafferty, C.N. and Clayton, R.K. (1978) Biochim. Biophys. Acta 502, 51–60.
21 Breton, J. (1985) Biochim. Biophys. Acta 810, 235–245.
22 Zinth, W., Kaiser, W. and Michel, H. (1983) Biochim. Biophys. Acta 723, 128–131.
23 Blasie, J.K., Erecinska, M., Samuels, S. and Leigh, J.S. (1978) Biochim. Biophys. Acta 501, 33–52.
24 Paillotin, G., Vermeglio, A. and Breton, J. (1979) Biochim. Biophys. Acta 545, 249–264.
25 Vermeglio, A., Breton, J., Barouch, Y. and Clayton, R.K. (1980) Biochim. Biophys. Acta 593, 299–311.
26 Eaton, W.A. and Hochstrasser, R.M. (1967) J. Chem. Phys. 46-7, 2533–2539.
27 Gao, J.L., Shopes, R.J. and Wraight, C.A. (1990) Biochim. Biophys. Acta 1015, 96–108.
28 Alegria, G. and Dutton, P.L. (1990) Biophys. J. 57, 571a.
29 Gunner, M.R. and Honig, B. (1990) in Perspectives in Photosynthesis, Jortner, J. and Pullman, B., eds.), pp. 53–60, Kluwer, Dordrecht.
30 Shill, D.A. and Wood, P.M. (1984) Biochim. Biophys. Acta 764, 1–7.
31 Rubin, A.B. and Devault, D. (1978) Biochim. Biophys. Acta 501, 440–448.
32 Bowyer, J.R. and Crofts, A.R. (1980) Biochim. Biophys. Acta 591, 298–322.
33 Alegria, G. and Dutton, P.L. (1991) Biochim. Biophys. Acta 1057, 239–257.